EUROPHYSICS LETTERS 1 August 2001

Europhys. Lett., **55** (3), pp. 362–368 (2001)

Field-induced anti-nematic ordering in assemblies of anisotropically polarizable particles

T. Bellini[1], M. Buscaglia[2], F. Leporati[3], F. Mantegazza[4] and A. Maritan[5]

[1] *INFM, Dipartimento di Fisica, Politecnico di Milano - 20133 Milano, Italy*
[2] *INFM, Dipartimento di Elettronica, Università di Pavia - 27100 Pavia, Italy*
[3] *INFM, Dipartimento di Informatica e Sistemistica*
Università di Pavia - 27100 Pavia, Italy
[4] *INFM, Dipartimento di Medicina Sperimentale*
Università di Milano Bicocca - 20052 Monza, Italy
[5] *INFM, SISSA - via Beirut 4, 34014 Trieste, Italy*

(received 8 February 2001; accepted in final form 28 May 2001)

PACS. 64.60.Fr – Equilibrium properties near critical points, critical exponents.
PACS. 82.70.Dd – Colloids.

Abstract. – We have investigated the effects of dipolar interactions in a lattice system of anisotropically polarizable particles in the presence of an external field both by Monte Carlo computer simulations and through a mean-field analysis. In a specific range of low temperature, large external field and large particle density, a novel staggered nematic structure is found, in which two intercalated sublattices have different nematic order parameters. First- and second-order phase transition lines, connected at a tricritical point, enclose the anti-nematic phase in the temperature-density plane.

Dipole-dipole coupling is not normally included among the basic processes governing phase stability and phase transitions in fluid systems. In some specific cases, though, dipolar interactions have been found to be at the origin of large-scale phase organization of soft matter. Accordingly, recent investigations by computer simulation [1] have focussed on the effects of permanent dipoles on molecular ordering. However, less attention has been devoted to electric-field–induced effects in fluids of highly polarizable entities [2]. In particular, induced-dipole–induced-dipole (ID-ID) interactions are expected to play a relevant role when other, typically stronger, interactions (steric, van der Waals, H-bonding) can be neglected. While this situation hardly occurs in simple molecular fluids, it is of relevance for instance when dealing with the orientational ordering in dispersions of electrically stabilized anisotropic particles. Being the electric polarizability of elongated polyelectrolytes huge and strongly anisotropic [3], ID-ID interactions are expected to produce, in such systems, dominant effects. Indeed, upon increasing the concentration of anisotropic charged colloids, an intriguing electro-optic phenomenon—first reported over 50 years ago [4]—is observed: the Kerr constant of the dispersion decreases and, in many cases, changes sign, indicating that, in the presence of an electric field, the particle axes are, on average, preferentially oriented perpendicularly to the field direction. To understand such "anomalous birefringence of polyelectrolytes"—so far basically unexplained—it is of crucial importance to explore in detail the contribution of the

ID-ID interactions to the orientational distribution in a system of rather dilute anisotropic particles. These considerations have inspired the simulation work here reported, in which we have examined a fairly simplified model which captures some peculiar features of this problem.

In this letter we offer evidence of a novel field-induced structure which is a specific consequence of ID-ID interactions. Specifically, we have considered a system of anisotropically polarizable spins on a lattice, in the presence of an external field E_0. The spins interact with each other only because of the induced electric dipoles they carry. The significant parameters of our study are E_0, the particle electric polarizability α, the temperature T and the system density. At high T, the system is in a "Para-Nematic" (PN) state, partially aligned along the field and invariant under rotations around the field direction. Upon decreasing T or increasing the density at constant E_0 and α, the system undergoes a spontaneous symmetry-breaking transition leading to an "Anti-Nematic" (AN) structure, where, in analogy to anti-ferromagnets, spins on two intercalated sublattices have different orientations. On one sublattice, the system has a high degree of orientational nematic order, while on the other one the spins lay perpendicular to the field without a preferred direction. Thus, the AN structure differs from the anti-ferromagnetic ordering because highly polarized spins are alternated with spins having small (induced) dipole rather than negative (permanent) dipole. At very low T a second novel "Anti-Tilt" (AT) phase is found, also characterized by different spin orientation on two intercalated sublattices. Namely, on both sublattices the spins are tilted away from the external field, but in opposite directions. Overall, the onset of the AN and AT ordering brings about a decrement of the mean alignment of the system with respect to what expected for non-interacting particles, in analogy with the experimental observations described above.

Our model system consists of N spins $\boldsymbol{s}_n$ ($n = 1, \ldots, N$) constrained on a cubic lattice, each of them characterized by a finite polarizability $\alpha_{||}$ along the spin axis and by a negligible perpendicular polarizability, *i.e.* the components of the polarizability tensor of the n-th spin, α_n, are $\alpha_n^{ij} = \alpha_{||} s_n^i s_n^j$, where s_n^i is the i-th component of the n-th spin. Under the effect of an external field the spins polarize and interact with each other via induced-dipole–induced-dipole interaction only. The (local) electric field at the n-th site, $\boldsymbol{E}_n^{\mathrm{loc}}$, is obtained by summing $\boldsymbol{E}_0$ and the dipolar field of the neighboring polarized spins (index m):

$$\boldsymbol{E}_n^{\mathrm{loc}} = \boldsymbol{E}_0 + \frac{1}{4\pi\varepsilon} \sum_{m \neq n} \frac{1}{\boldsymbol{r}_{nm}^3} \big((3\alpha_m \cdot \boldsymbol{E}_m^{\mathrm{loc}}) \cdot \boldsymbol{u}_{nm} \boldsymbol{u}_{nm} - \alpha_m \cdot \boldsymbol{E}_m^{\mathrm{loc}} \big), \tag{1}$$

where ε is the dielectric constant of the medium hosting the particles and $\boldsymbol{u}_{nm}$ is a unit vector along the line joining the n-th and m-th site whose mutual distance is $\boldsymbol{r}_{nm}$. The Hamiltonian of the system is

$$H = -\frac{1}{2} \sum_n \big(\alpha_n \cdot \boldsymbol{E}_n^{\mathrm{loc}} \big) \cdot \boldsymbol{E}_n^{\mathrm{loc}} = -\frac{\alpha_{||}}{2} \sum_n \big(\boldsymbol{s}_n \cdot \boldsymbol{E}_n^{\mathrm{loc}} \big)^2. \tag{2}$$

The equilibrium configuration of the system described by eqs. (1) and (2) is difficult to intuitively predict because of the competing effect of the external field, favoring parallel alignment, and of dipolar interactions, favoring parallel head-tail configurations but anti-parallel side-side alignment. We have thus investigated this model by performing Monte Carlo Metropolis computer simulations. Analysis of eqs. (1) and (2) reveals that in the simulation there are two relevant and independent dimensionless parameters: $\tau = k_{\mathrm{B}}T/\alpha_{||}E_0^2$ and $\rho = \alpha_{||}/(4\pi\varepsilon d^3)$, where $k_{\mathrm{B}}T$ is the thermal energy and d is the lattice unit length. τ gauges the coupling with the external field while ρ, proportional to the particle density, controls the strength of the dipolar interaction.

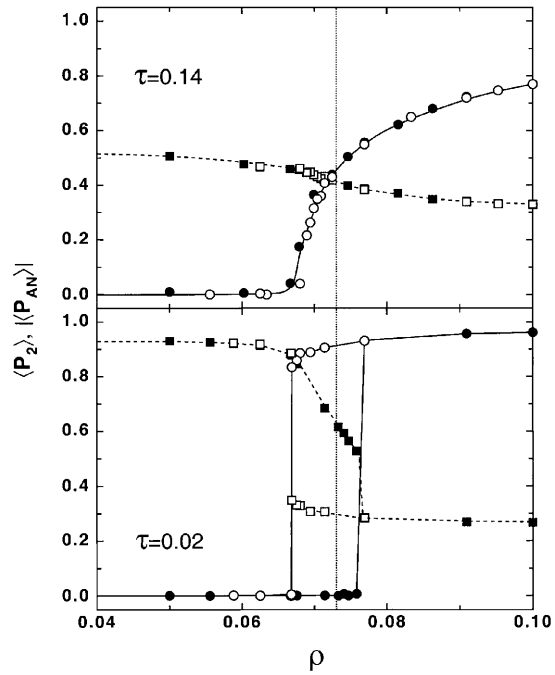

Fig. 1 – Nematic order parameter $\langle P_2 \rangle$ (squares) and anti-nematic order parameter $|\langle P_{\rm AN} \rangle|$ (dots) obtained by Monte Carlo simulations at $\tau = 0.14$ and $\tau = 0.02$ for various values of ρ, the average being typically on 10^4 macrosteps. Full and open symbols indicate the values obtained by equilibrating the system from different initial conditions: spins initially aligned in the z-direction, *i.e.* $\langle P_2 \rangle = 1$ (full symbols); spins initially aligned as a perfect AN, *i.e.* $P_{\rm AN} = 1$, $P_2 = 0.25$ (open symbols). The dotted line marks the position $\rho_{\rm AN,0} \approx 0.073$. Lines through the data have been added to guide the eyes.

Given the invariance of eqs. (1) and (2) for local spin inversion, the average spin orientation is $\langle \boldsymbol{s}_n \rangle = 0$ always, while the lowest-order non-vanishing quantity gauging the induced orientational order is the nematic order parameter $P_2 = \frac{1}{2N} \sum_n (3 \cos^2 \vartheta_n - 1)$, ϑ_n being the angle between the n-th spin and E_0. In the limit of high dilution the particles are independent and P_2 can be simply derived from the Boltzmann angular distribution $f(\vartheta) = \exp[\frac{\cos^2 \vartheta}{2\tau}]$.

To simplify matters, in the simulation we have limited our calculations based on eq. (1) to nearest neighbors only. Despite the simplification, the recursive implicit nature of eq. (1), expressing the mutual induction interaction among the spins, makes it impossible to compute $\boldsymbol{E}_n^{\rm loc}$ at any site without having determined the entire set $\{\boldsymbol{E}_n^{\rm loc}\}$ of local field amplitude and orientation on all sites. Accordingly, to calculate the energy—and thus apply the Metropolis criterion—after every move we have performed a set of cycles at fixed spin orientations, during which $\{\boldsymbol{E}_n^{\rm loc}\}$ are computed using eq. (1) on the basis of the local fields obtained in the previous cycle [2]. Typically, ten such recursive "dipole equilibration" cycles were enough to ensure that the system energy was defined with a precision better than $10^{-3} k_{\rm B} T$. In a 10^3 lattice, this procedure increases the computational time by about 1000 times with respect to standard models where the energy is an explicit function of spin orientations [5]. This is why we performed simulations on lattices of 10^3 spins, smaller than in typical Heisenberg or Lebwhol-Lasher model simulations [6].

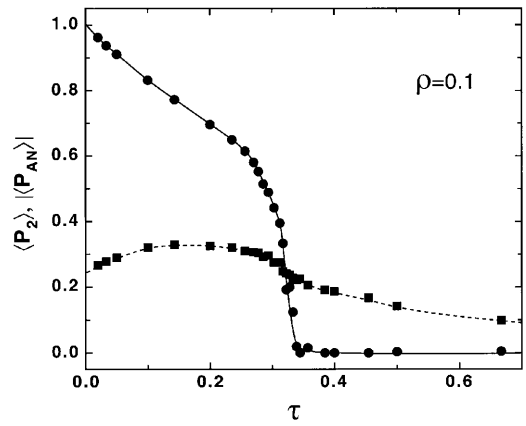

Fig. 2 – Nematic order parameter $\langle P_2 \rangle$ (squares) and anti-nematic order parameter $|\langle P_{\rm AN} \rangle|$ (dots) obtained by Monte Carlo simulations for $\rho = 0.1$ and various values of τ. Initial condition of fully aligned spins, *i.e.* $\langle P_2 \rangle = 1$, were employed. Lines through the data have been added to guide the eyes.

We have performed simulations for different choices of τ and ρ, using a perfectly aligned sample as the initial condition. In fig. 1 we show (full squares) the dependence of the mean orientation $\langle P_2 \rangle$ on the coupling strength ρ for $\tau = 0.14$ and for $\tau = 0.02$. Averages have been performed at equilibrium on typically 10^4 macrosteps. In both cases $\langle P_2 \rangle$ is a decreasing function of ρ, continuous if $\tau = 0.14$ and discontinuous if $\tau = 0.02$. In both cases, for $\rho \sim 0.1$, $\langle P_2 \rangle \sim 0.3$. Larger values of ρ cannot be explored because ρ is intrinsically limited by the requirement that any particle cannot polarize more than what needed to cancel its internal field. For spherical particles of radius $d/2$ on a cubic lattice, this sets $\rho_{\rm max} = 1/8$. Indeed, when $\rho > 0.125$, the simulation is unstable: the dipolar field becomes self-sustained, yielding diverging values of $\boldsymbol{E}_n^{\rm loc}$ during the dipole equilibration cycles. In fig. 2 we show (squares) $\langle P_2 \rangle$ *vs.* τ for $\rho = 0.1$. Notice the non-monotonic behavior and that $\langle P_2(\tau \to 0) \rangle \sim 0.25$. Thus, in both figs. 1 and 2, we observe that a significant reduction of the orientational order takes place in regimes where the ID-ID interaction dominates, *i.e.* at low τ and high ρ. The origin of this phenomenon is more apparent when inspecting the snapshots of equilibrium configurations, as those presented in fig. 3. Panels 3A and 3B both refer to $\tau = 0.02$ and $\rho = 0.1$ and show, respectively, a projection of the whole lattice on the xy-plane and a xz section of the lattice, z being the direction of E_0. Let us identify each spin by the triplet $\{i, j, k\}$ of its coordinates, expressed in units of d. Figures 3A and 3B clearly show that a dramatic transformation has taken place: the system has spontaneously split into two intercalated sublattices, identified by $i + j$ being even or odd. Both sublattices maintain the rotational symmetry around the z-axis ($\langle s_x \rangle = \langle s_y \rangle = 0$) but display different degrees of nematic order. Panel 3C shows the snapshot of a yz section obtained at equilibrium for $\tau = 0.01$ and $\rho = 0.085$, where an AT structure is found. As visible from the figure, in the AT ordering the spins are tilted with respect to the z-axis, the tilt being, for the whole system, either in the xz- or in the yz-plane. The tilt has the same amplitude but different directions on two intercalated sublattices arranged to form a chessboard when the lattice is cut along the plane including z and perpendicular to the tilt plane (yz in the case of fig. 3C. Thus, the AT structure is the result of two distinct symmetry breakings: the tilt takes place in one of the two equivalent planes xz and yz; spin tilt toward the positive x (or y) is found on one of two equivalent sublattices, identified by $i + k$ (or $j + k$) being either even or odd.

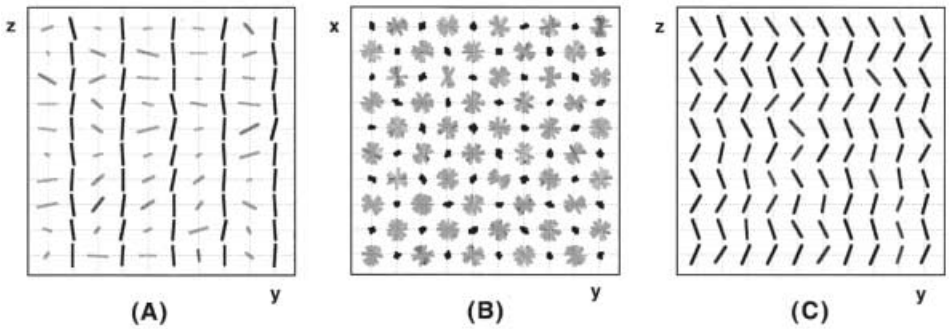

Fig. 3 – Snapshots from the equilibrium state obtained for $\tau = 0.02$ and $\rho = 0.1$ (A and B) and for $\tau = 0.01$ and $\rho = 0.085$ (C). Snapshots A and C show a yz section of the lattice; snapshot B is obtained as a projection of the whole lattice on the xy-plane. The segments represent as the projection of spins of length 0.8 lattice units. A gray scale has been used to give notice to different ϑ values. Notice, in panel B, the chessboard-like organization of orientations, the defining property of the AN phase. An analogous chessboard organization of positive and negative tilt is found by cutting the AT phase in the snapshot C along the xz-plane.

In order to quantify the degree of staggered nematic order depicted in fig. 3, we introduce the AN order parameter P_{AN}, defined as the difference between P_2 evaluated in the two sublattices (a and b), and normalized to take values in the interval $(-1, 1)$:

$$P_{\mathrm{AN}} = \frac{2}{3}\big(P_2^{\mathrm{a}} - P_2^{\mathrm{b}}\big) = \frac{2}{3N}\sum_{i,j,k}(-1)^{i+j}\big(3\cos^2\vartheta_{ijk} - 1\big). \tag{3}$$

Figures 1 and 2 (dots) indicate that this definition of P_{AN} well captures the symmetry of the AN order, and show that different transitional behaviors are obtained for different choices of parameters. Specifically, the ρ-dependence of $|\langle P_{\mathrm{AN}}\rangle|$ indicates that the onset of the AN ordering takes place through a discontinuous first-order phase transition at low τ and through a continuous second-order phase transition at larger τ. The nature of the phase transitions is confirmed when simulation performed with different initial conditions are compared. The values of $|\langle P_{\mathrm{AN}}\rangle|$ (and $\langle P_2\rangle$) obtained from simulations evolving from either an aligned sample (full symbols) and from a "perfect" AN configuration (open symbols) well match for $\tau = 0.14$ (fig. 1a) but not for $\tau = 0.02$, in which case hysteresis due to metastability is found (fig. 1b). In fig. 4 we show (dots) the phase transition line in the (ρ, τ)-plane as determined from the simulations. The first- and second-order transition lines merge at the point TP, which we therefore identify as a tricritical point. Given the symmetry of the problem, analogous to the uniaxial antiferromagnets, we expect the second-order PN-AN phase transition to be characterized, far enough from TP, by the critical exponents of the 3D Ising symmetry class [7].

Seeking further confirmation to our observations, we have considered the $\tau = 0$ limit, in which analytical calculations of H are possible. In fig. 1 we have marked by a vertical line the value of $\rho_{\mathrm{AN},0}$, the PN-AN transition density at $\tau = 0$, calculated by locating the density at which the energy of the perfectly aligned system and of the perfect AN state are equal. The calculation yields $\rho_{\mathrm{AN},0} = 0.072$, nicely matching the $\tau = 0.02$ simulation results. The neglect of entropic contributions, inherent in the $\tau = 0$ calculations, makes it possible to calculate $\rho_{\mathrm{AN},0}$ by taking into account the interactions with neighbors at higher order. Considering interactions between spins up to 4 lattice unit lengths (sufficient to stabilize the result), we obtain $\rho_{\mathrm{AN},0} = 0.109$. We have also calculated, at $\tau = 0$, the effect of including the transversal

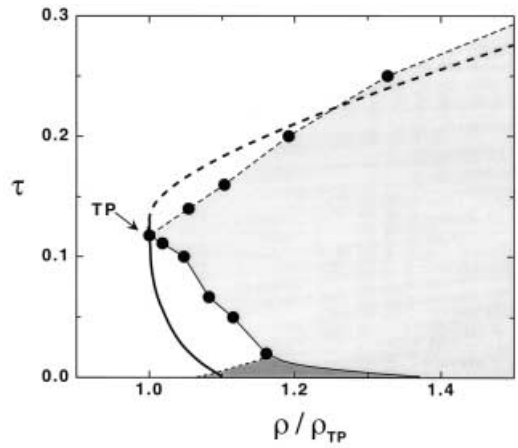

Fig. 4 – Phase diagram of the PN (white), AN (light gray) and AT (dark gray) phases in the (ρ, τ)-plane as obtained by computer simulation (dots). The ρ interval for the AT phase has been set by $\tau = 0$ calculations. Thick lines indicate the PN-AN phase boundary according to the mean-field analysis. Continuous and dashed lines indicate, respectively, first- and second-order phase transitions. All data have been scaled with respect to the density ρ_{TP} of the tricritical point: $\rho_{\mathrm{TP}} = 0.06$ for computer simulations and $T = 0$ calculations; $\rho_{\mathrm{TP}} = 0.113$ for mean-field analysis.

polarization, $\alpha_\perp$, previously neglected. Upon increasing the value of $\alpha_\perp$, and keeping all the other parameters fixed, the value $\alpha_{||} - \alpha_\perp$ needed to induce AN ordering decreases. For example, in the case in which $\alpha_{||}/\alpha_\perp = 3$ (as in the case described in ref. [3]), and defining, in this case of partial anisotropy, $\rho = (\alpha_{||} - \alpha_\perp)/(4\pi\varepsilon d^3)$, we find $\rho_{\mathrm{AN},0} = 0.053$. This analysis confirms that the AN phase is neither a consequence of neglecting non-nearest neighbors, nor an artifact due to the $\alpha_\perp = 0$ assumption, but rather a remarkable effect of the symmetry of the induced dipole interaction. Moreover, the $\tau = 0$ analysis also indicates that the AT phase is energetically favored over both the PN and AN phases in the interval $0.063 < \rho < 0.082$. The presence of the AT phase at $\tau = 0.01$ and its absence at $\tau = 0.02$ suggests that such a phase is entropically unfavorable, as could be expected from its loss of rotational symmetry around z.

To better understand the nature of the AN phase, we have studied the model in mean-field approximation on the basis of H_{s}, a simplified version of the H obtained by solving eq. (1) for $\boldsymbol{E}_n^{\mathrm{loc}}$ through a first-order expansion in ρ:

$$H_{\mathrm{s}} = -\frac{\alpha_{||}}{2}\sum_n (\boldsymbol{s}_n \cdot \boldsymbol{E}_0)^2 - 2\alpha_{||}\rho \sum_{nm} \big[3(\boldsymbol{s}_n \cdot \boldsymbol{E}_0)(\boldsymbol{s}_n \cdot \boldsymbol{u}_{nm})(\boldsymbol{s}_m \cdot \boldsymbol{u}_{nm})(\boldsymbol{s}_m \cdot \boldsymbol{E}_0) - (\boldsymbol{s}_n \cdot \boldsymbol{E}_0)(\boldsymbol{s}_n \cdot \boldsymbol{s}_m)(\boldsymbol{s}_m \cdot \boldsymbol{E}_0)\big]. \tag{4}$$

A variational estimate of the free energy for the model in eq. (4) can be obtained in the standard mean-field approximation (see, *e.g.*, ref. [7]) using a trial Hamiltonian $H_0 = \sum_n \boldsymbol{s}_n h_n \boldsymbol{s}_n$, where h_n is a 3×3 matrix. In order to study the PN-AN transition h_n has been chosen to depend only on the two sublattices referred above. Analysis of such a free energy leads to the phase diagram in the (ρ, τ)-plane shown in fig. 4 by thick lines. Its noticeable features are: i) the presence of both first-order (dashed line) and second-order (dotted line) phase transitions; ii) the resulting existence of a tricritical point, located at the lowest ρ at which the AN phase is found; iii) the negative slope of the first-order transition line, attesting

a re-entrant behavior of the AN phase in a limited ρ interval. This last feature indicates that, in such ρ interval, the AN phase is promoted by entropy over the PN phase. Overall, the phase diagram obtained through the mean-field analysis well agrees with the simulation results in all the relevant features, confirming the remarkable potential of the induced-dipole–induced-dipole interaction in the formation of new phases in systems of highly anisotropic particles.

In conclusion, this paper constitutes the first study of the effects of the interactions between induced dipoles on the orientational order of particles having anisotropic polarizability. This problem has been tackled by studying a spin lattice model through calculations at $\tau = 0$, Monte Carlo Metropolis computer simulations, and mean-field analysis. All level of investigation indicate the onset, at low temperature and high enough density, of a new kind of orientational ordering, the AN order, here introduced for the first time. The $\tau = 0$ analysis, which includes high-order neighbor interactions and partial anisotropy, confirms the AN phase as an intrinsic consequence of the ID-ID interaction in an ordered system of spins. The Monte Carlo Metropolis investigation, performed on the simplified model where spins having $\alpha_\perp = 0$ interact at the nearest-neighbor level, has revealed a rich phase diagram, featuring both continuous and discontinuous phase transitions. The richness is confirmed by the mean-field analysis, performed on a further simplified model, which yields an AN phase diagram featuring first- and second-order transition lines, a tricritical point and re-entrant behavior. Comparison of the results here presented with real fluid systems requires studying the effects of the ID-ID interactions in geometries other than the cubic lattice, possibly less compatible with the simple AN ordering.

* * *

We thank M. Glaser and C. Zannoni for useful discussions and L. Brambilla for computer support.

REFERENCES

[1] Kiyohara K., Gubbins K. E. and Panagiotopoulos A. Z., *Mol. Phys.*, **94** (1998) 803; Berardi R., Orlandi S. and Zannoni C., *Chem. Phys. Lett.*, **261** (1996) 357.
[2] Hloucha M. and Deiters U. K., *Fluid Phase Equil.*, **149** (1998) 41.
[3] Bellini T., Mantegazza F., Degiorgio V., Avallone R. and Saville D. A., *Phys. Rev. Lett.*, **82** (1999) 5160.
[4] O'Konski C. T. and Zimm B. H., *Science*, **111** (1950) 113; Cates M. E., *J. Phys. (Paris)*, **19** (1992) 1109; Radeva T., Peikov V., Stoylov S. P. and Hoffmann H. H., *Coll. Surf.*, **119** (1996) 1, and references therein; Kramer H. *et al.*, *J. Phys. II*, **4** (1994) 1061, and references therein.
[5] Danese G. *et al.*, *Comput. Phys. Commun.*, **134** (2001) 47.
[6] Frenkel D. and Smit B., *Understanding Molecular Simulations. From Algorithms to Applications* (Academic Press, San Diego) 1996.
[7] Chaikin P. M. and Lubensky T. C., *Principles of Condensed Matter Physics* (Cambridge University Press, Cambridge) 1995.